# Evolutionary public goods game on the birandom geometric graph

Yang Li,[1] Hao Sun,[1,*] Weibin Han,[2] and Wanda Xiong[1]
[1]*Department of Applied Mathematics, Northwestern Polytechnical University, Xi'an 710129, China*
[2]*School of Economics and Management, South China Normal University, Guangzhou 510006, China*

(Received 5 January 2020; accepted 23 March 2020; published 15 April 2020)

To investigate the evolution of cooperation in spatial public goods games, this paper establishes a birandom geometric graph, in which two types of nodes, representing players and public goods respectively, are placed at random locations in the unit square. Each public good has a limit influence range and the individuals that fall into the same range engage in a public good game. In contrast to the classical network models consisting of only one type of nodes, the birandom geometric graph provides a natural way to describe the scenarios where individuals and public resources are independent of each other. Numerical simulations reveal that cooperation can be significantly promoted when the group size and the average number of groups that each player participates in are relatively small, which is at odds with the results on the square lattice, but is consistent with a body of empirical evidence reported by Ostrom and Olson *et al.* Analysis of the evolutionary process suggests that the facilitation of cooperation is due primarily to the formation of the cooperative clusters, which can effectively resist the invasion of the defectors.

DOI: 10.1103/PhysRevE.101.042303

## I. INTRODUCTION

In many social and economic organizations, individuals are confronted with conflicts between their own interests and collective interests. Hardin's *The Tragedy of the Commons* indicated that these conflicts can lead to overexploitation and collapse of public resources [1]. However, altruistic behaviors among self-interested individuals extensively exist, which poses a riddle. Thus many empirical and theoretical studies have been performed to explore the reasons for the emergence of cooperation. Olson [2] pointed out that the greater effectiveness of relatively small groups is evident from observation and experience. Coincidentally, Ostrom [3,4], who became the first woman to receive the prestigious Nobel Prize in Economics for her research in the management of public resources, concluded from empirical research that a cooperative organization will come into existence if the group size is relatively small and the users live perennially near common-pool resources, which agrees well with the results obtained in the following sections of this paper.

In terms of theoretical research, as a powerful mathematical framework, evolutionary game theory [5–11] is widely applied to study social dilemmas. In particular, the public goods game (PGG) for group interactions has attracted much attention [12,13]. In a typical PGG, each player must decide simultaneously whether to contribute (cooperate) or not (defect) to the common pool. The accumulated contribution is multiplied by an enhancement factor and then evenly redistributed across all participants, irrespective of their initial decision. Obviously, a defector can obtain a higher payoff by exploiting the cooperative efforts of others, which leads to the deterioration of cooperation [14]. To explore how cooperative behavior evolves among selfish individuals, several mechanisms have been put forward over the last decades [15–28]. Network reciprocity, as one of the five rules discussed in Ref. [29], is known to play a critical role in the evolution of cooperation. A pioneering work performed by Szabó *et al.* [30] analyzed the voluntary participation in the PGG on a square lattice and found that optional participation can efficiently prevent successful spreading of selfish behavior. Considering diversity is ubiquitous, Santos *et al.* [31] introduced social diversity by means of heterogeneous graphs and concluded that cooperation was enhanced by the diversity associated with the number and size of the PGGs. Moreover, Rong *et al.* [32] studied the influence of degree correlation on the evolution of cooperation in the networked PGG. With the aid of a double-star graph, they noticed that the assortative mixing among the individuals inhibits the emergence and sustainment of the cooperation. Additionally, Szolnoki *et al.* [33] investigated the spatial effect on the square lattice and focused on the effects of different sizes of groups. Simulation results indicated that cooperation may be promoted by means of enhanced spatial reciprocity that sets in for very large groups. Following this line, many modified PGG models have been studied on various typical complex networks, such as regular lattices, small-world networks and scale-free networks, etc.

However, almost all the existing network models employed to study the spatial PGG consist of only one kind of nodes, that is, each node represents both a public good and a player. Such models cannot accurately characterize the interaction structure between individuals in reality, because it is obvious that players and public goods are independent of each other. More intuitively, both natural resources (such as mineral, fishing) and communal facilities (such as parks, roads) can be regarded as public goods, but they are not tied to some

*Corresponding author: hsun@nwpu.edu.cn

 

people. Meanwhile, it should be noted that the connections between users of public resources are usually based on spatial location rather than social relationships, just as you can not be acquainted with everyone in a park, the reason why you are enjoying the same public resource is that you are within its service range.

These facts challenge the common assumption that each individual engages in the PGGs centered on his neighbors and himself. Therefore, we propose a novel network model, called birandom geometric graph (BRGG), in which public goods and individuals are, respectively, represented by two kinds of nodes that randomly sampled from the uniform distribution of underlying space $[0, 1]^2$. We assume that each public good has a circular service range with an adjustable radius and the players that fall into the same range participate in a PGG. In this case, the structure of the network is mainly determined by group size and the number of groups per capita participation. This paper focus on clarifying the effects that are brought about by the network structure on the evolution of cooperation. Large quantities of simulations demonstrate that, when the group size and the number of groups that each individual partakes in are relatively small, cooperation can be significantly promoted even in the absence of reputation, punishment, preferential selection, and other mechanisms. Our results differ from the conclusions of evolutionary PGG on regular networks [33], but are in accord with many empirical results exhibited by Ostrom. In addition, the BRGG provides a potentially promising avenue to capture the complex relationships of the users of public resources.

The remainder of this paper is structured as follows. The details of our model will be presented in Sec. II. We discuss the results of computer simulations in Sec. III and summarize our findings in Sec. IV.

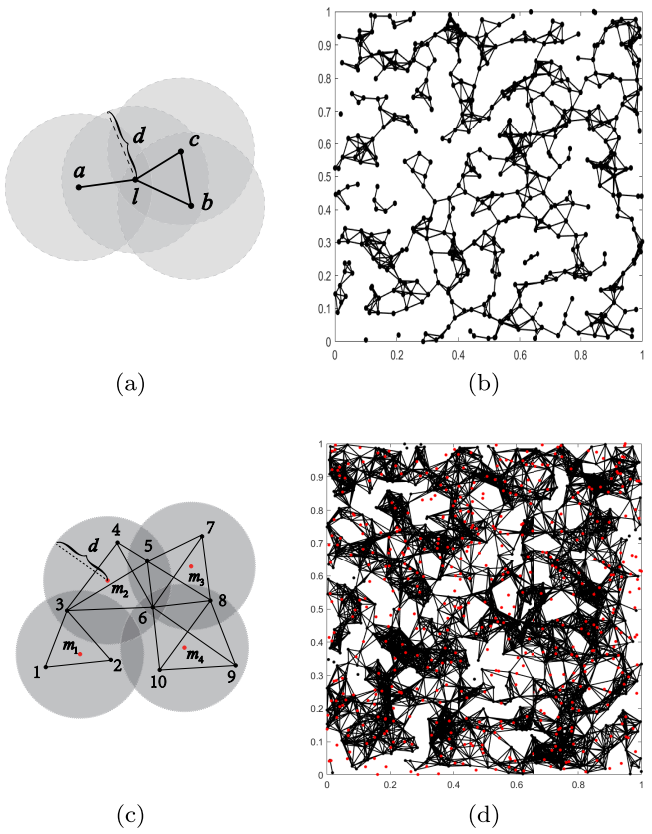


FIG. 1. Top row: illustration of the RGG's vertex attachment rule is shown in (a). A standard RGG in the domain $[0, 1]^2$, with $N = 1000$ and $d = 0.05$, shown in (b). Bottom row: the schematic diagram of BRGG is shown in (c). A BRGG with $M = 500$ and $N = 1000$ is shown in (d), where the fixed radius $d$ is 0.05. The red vertices representing common resources and the black vertices representing players. There are no edges across the boundaries, i.e., the boundary conditions are open, not continuous.

## II. MODEL

The theory of random geometric graphs (RGGs) enables research of complex networks via geometry [34,35]. The standard RGG is a graph where $N$ nodes are placed at random location in the unit square, and attached to others nodes within distance $d$, as shown in Figs. 1(a) and 1(b). The properties of networks generated along this way have been exhaustively studied, with particular emphasis on percolation [36,37].

Inspired by RGG, we propose the concept of BRGG, which is composed of two types of nodes, namely public good nodes and player nodes. Initially, $M$ public good nodes are assigned random coordinates in $[0, 1]^2$ and each public good node $m_i$ has a circular influence zone with radius $d$. Player nodes arrive at a rate of one per unit time, they are also placed at random locations in the same square and attached to all exiting player nodes in the same zone. The process stops until $N$ player nodes are present in the network [see Figs. 1(c) and 1(d) for an illustration]. For given $M$, $N$, and $d$, the average number of players per group is $z = \pi d^2 N$, and the average number of groups per capita is $y = \pi d^2 M$. The variation of network structure is closely related to parameters of $z$ and $y$. Note that varying $M$, $N$, and $d$ but keeping $z$ and $y$ fixed will cause networks to have the similar structures. Besides, varying $d$ but keeping $M$ and $N$ fixed, i.e., changing $z$ and $y$, the networks generated will have very different statistical properties; if $d \ll 1$, large numbers of isolated nodes will exist; if $d > 1$, the network will be fully connected. Ideally, for the sufficiently large value of $M$, altering the values of $N$ and $d$ will enable most network structures to be represented. There is no in-depth study on the specific properties of BRGG, and it is not the focus of this paper.

To explore the evolutionary PGG on the BRGG, simulations are carried out on the BRGG with $M$ public goods and $N = \alpha M$ players, where $\alpha$ is the ratio of the number of players to public goods. Initially, each individual $i$ is designated as a cooperator ($s_i = 1$) or defector ($s_i = 0$) with equal probability. In our model, players contribute and receive payoffs from the PGGs centered on public goods instead of their neighbors. Therefore, an indicator function $\delta_{i,l}$ is introduced to indicate whether $i$ is in the group $G_l$ centered on the public good node $l$,

$$\delta_{i,l} = \begin{cases} 1, & i \in G_l, \\ 0, & i \notin G_l. \end{cases} \tag{1}$$

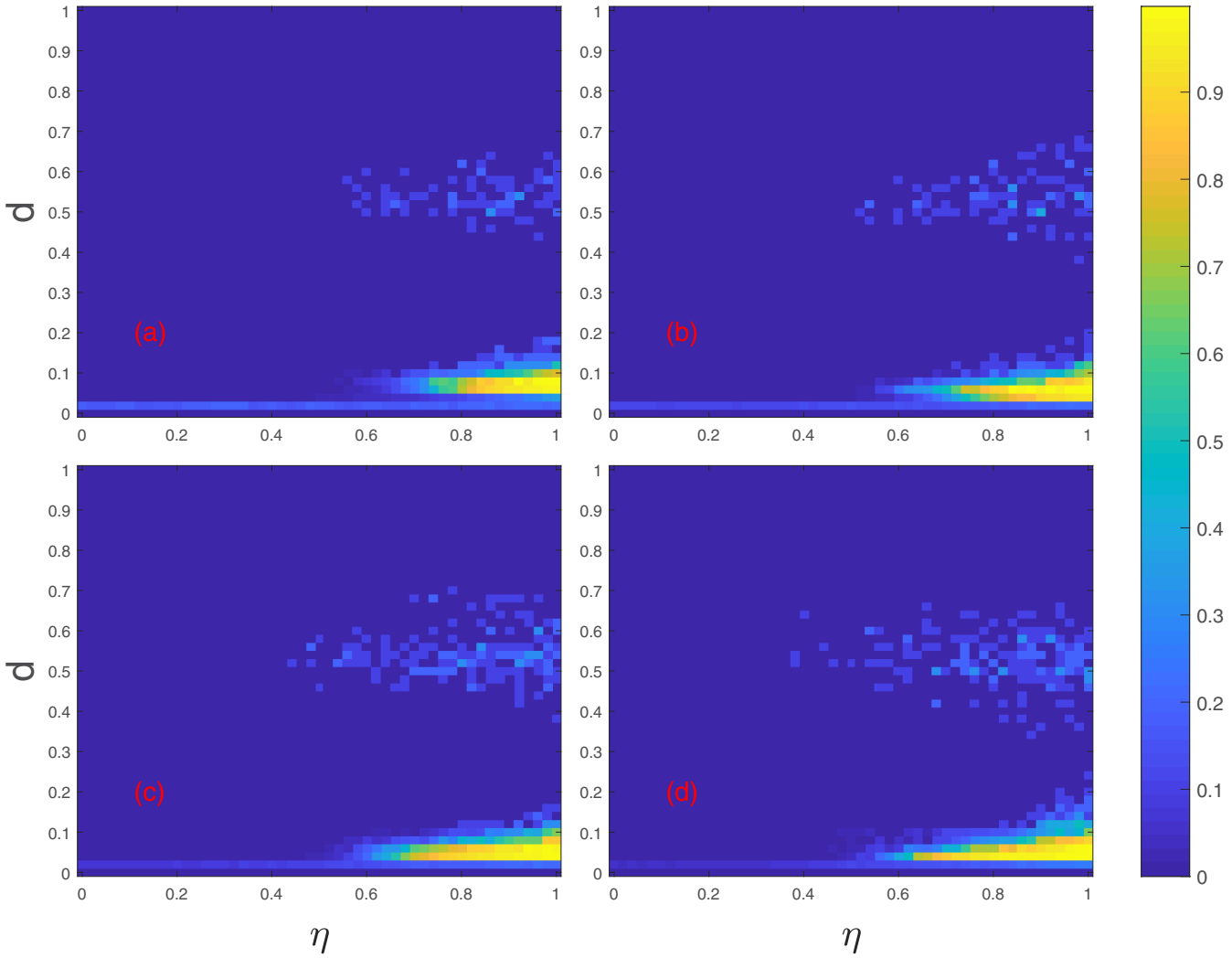


FIG. 2. Fraction of cooperators $\rho_C$ in the equilibrium state as a function of $d$ and $\eta$ for different values of $\alpha$. From (a)–(d), $\alpha$ is set to be 0.5, 1.0, 1.5, 2.0. There are no edges across the boundaries, i.e., the boundary conditions are open, not continuous. Other parameter setup is $M = 1000$, MCS $= 10000$, $\kappa = 0.1$.

Specifically, isolated players are not counted in the results. Then, player $i$'s payoff from group $G_l$ is

$$P_{i,l} = \frac{r\sum_j^N \delta_{j,l}s_j}{\sum_j^N \delta_{j,l}} - s_i, \tag{2}$$

where $\sum_j^N \delta_{j,l}$ is the size of the group $G_l$ and $\sum_j^N \delta_{j,l}s_j$ denotes the number of cooperators in $G_l$. $r$ stands for the enhancement factor. Therefore, the total payoff of player $i$ can be summed up as

$$P_i = \sum_{l=1}^{M} P_{i,l}. \tag{3}$$

After obtaining the total payoff, each individual $i$ will adjust its strategy by replicating the strategy of a randomly selected neighbor $j$ with a probability

$$W(s_i \leftarrow s_j) = \frac{1}{1+\exp[(P_i - P_j)/\kappa]}, \tag{4}$$

where $\kappa$ characterizes the environmental noise and $P_i$ represents $i$'s total payoff [38,39]. In line with most previous studies, we set $\kappa$ to be 0.1 [30,31,40].

In the process of evolution, on the one hand, given that the distribution of public goods in real life and the scope of people's activities are bounded (such as cities and villages), simulations are carried out on the BRGG with aperiodic boundary. The size of the network is $M = 1000$, and $\alpha$ is set to be 0.5, 1.0, 1.5, 2.0, respectively. As a comparison, we also present results under periodic boundary conditions. On the other hand, we explore the impact of different sizes of BRGGs on the cooperation level (e.g., $M = 200$, 500, and 1000), and the consequences are consistent with the above conclusions about the characters of the network structure.

The level of cooperation is characterized by the fraction of cooperators $\rho_C$, which is defined as the ratio of the cooperators to the participations in the steady state. In the following simulations, $\rho_C$ is obtained by averaging over the last 1000 steps of the up to $10^4$ Monte Carlo steps (MCS). Each data results from an average of over 20 realizations. In addition, isolated nodes will inevitably appear due to the random distribution of nodes.

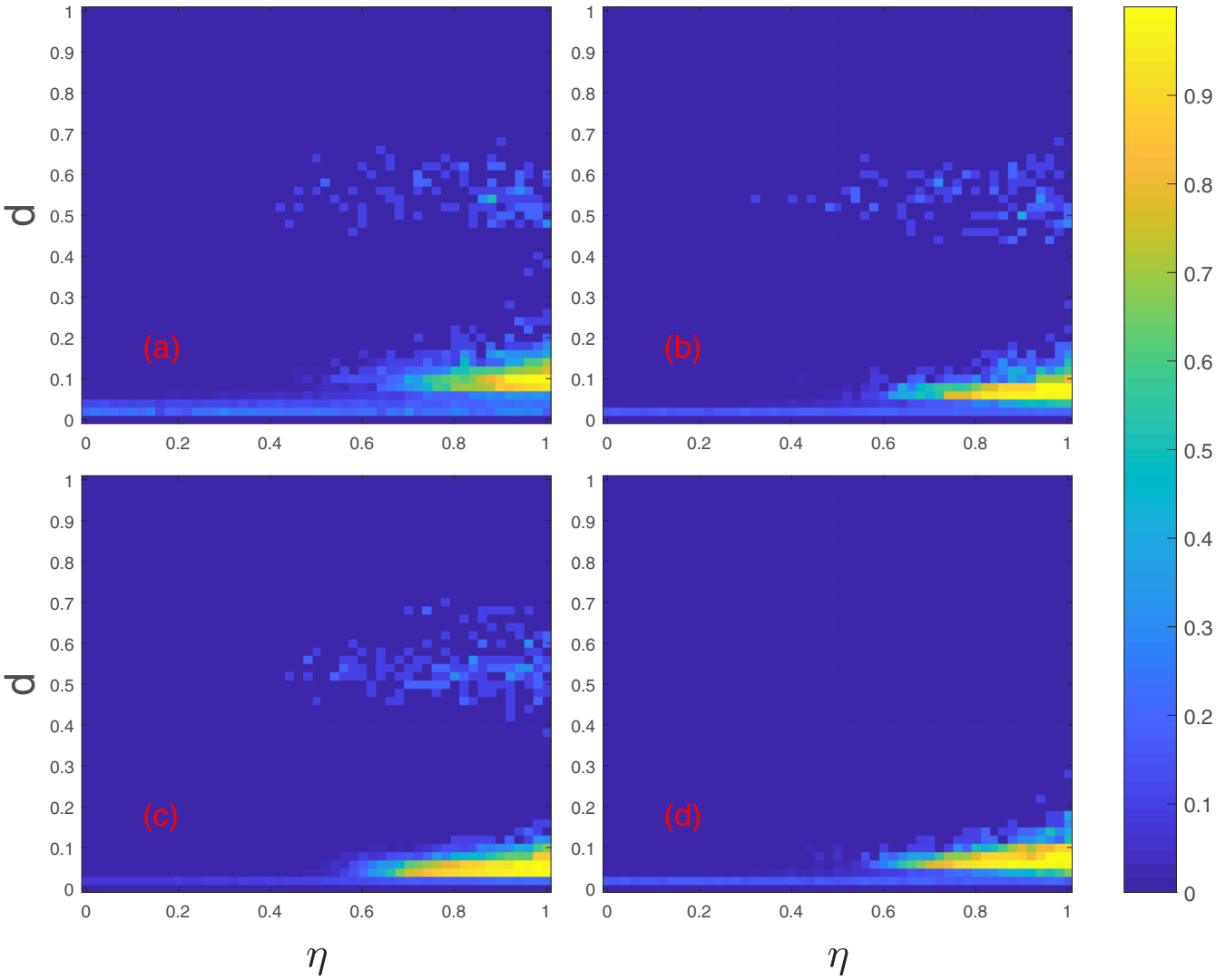


FIG. 3. Fraction of $\rho_C$ at the stationary state as a function of $d$ and $\eta$ for various sizes of network. From (a)–(c), $M$ is set to be 200, 500, 1000, respectively, and the boundary conditions are open. In (d), $M$ is equal to 500, and the boundary conditions are continuous. Other parameter setup is $\alpha = 1.5$, MCS $= 10000$, $\kappa = 0.1$.

Nevertheless, a large number of simulations have verified that in the case of $M = 1000$, when $d > 0.02$, the proportion of loners is less than 1% and decreases rapidly as $d$ increases.

### III. SIMULATION AND ANALYSIS

To begin with, we present the fraction of cooperators $\rho_C$ as a function of the service radius $d$ and the normalized enhancement factor $\eta = r/z$ for different values of $\alpha$ in Fig. 2, where $z$ is the average number of players per group. As one can see that cooperators can survive the evolution for different combinations of $d$ and $\eta$ in the absence of reputation, punishment and preferential selection, etc. It is worth pointing out that the distribution of data points with $\rho_C > 0$ is bimodal. Take $\alpha = 0.5$ for an example, high level of cooperation can be achieved for small values of service radius (when $0.04 < d < 0.12$), but the range of parameter $d$ that leads to high level of cooperation is small. For the intermediate values of service radius (when $0.44 < d < 0.64$), the maximum level of cooperation is less than 0.3, but parameter $d$'s range is wider than the former. In other cases, the defectors dominate the entire system. It can also be seen from Fig. 2 that the boundary between the parameter area of high-level cooperation and the area of complete defection is blurred. Due to quenched spatial randomness, the phase transitions become relatively slow in the vicinity of critical points (these features are more clearly shown in Fig. 4 and Fig. 5). The rigorous analyses of these critical phenomena are well investigated in Refs. [11,41], which do not belong to the scope of the present study. The numerical analyses of this paper are focused on deriving simple phase diagrams.

Figure 3 presents comparison results of $\rho_C$ under different values of $M$. From Fig. 3(a)–3(c), $\alpha$ is fixed to be 1.5 and $M$ is set to be 200, 500, 1000, respectively. We find that as $M$ increases, the value of $d$ that reaches the same level of cooperation will decrease, which implies that if $M$ is improved, $d$ will be correspondingly reduced in order to keep the network structure unchanged. The simulation results agree well with the conclusion as stated in the previous section and it also indicates that increasing group size and the average

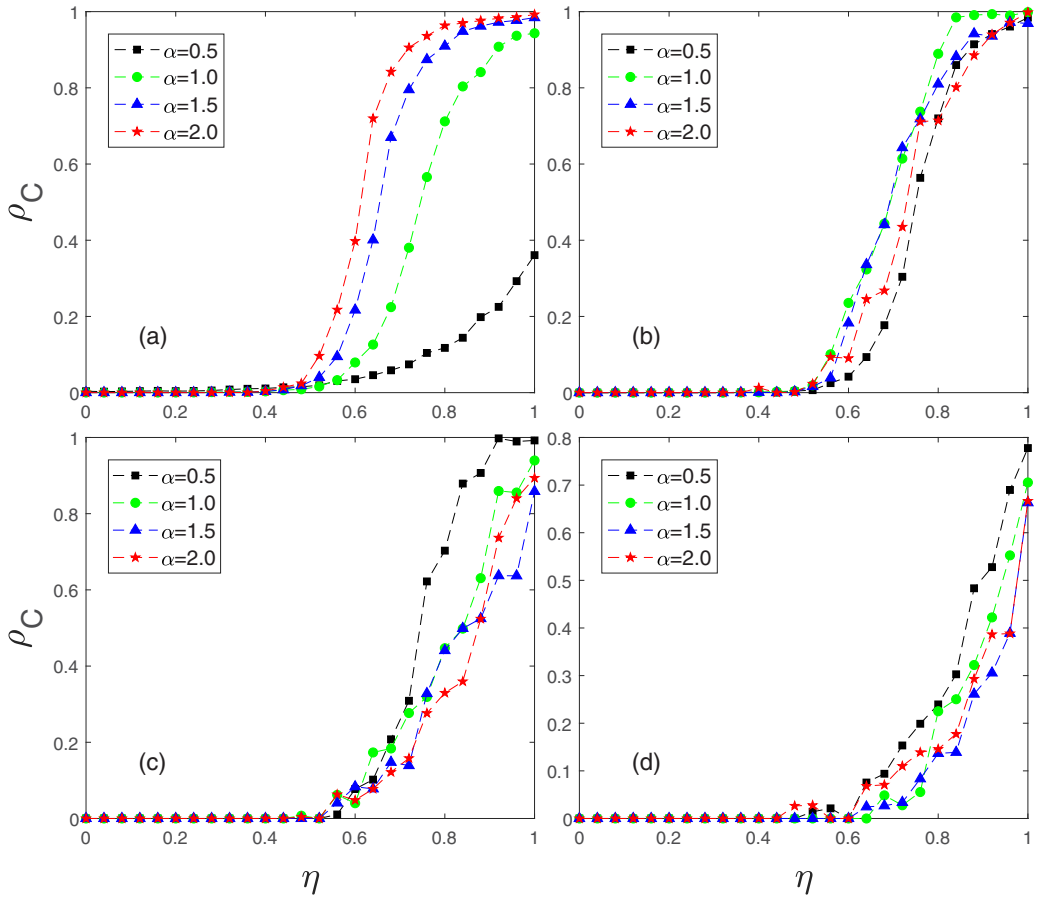


FIG. 4. Fraction of cooperators $\rho_C$ at the stationary state as a function of the normalized enhancement factor $\eta$ for different values of $\alpha$. From (a)–(d), the service radius $d$ is set to be 0.04, 0.06, 0.08, 0.10, respectively. In each panel, the $\alpha$ is changed from 0.5 to 2.0. Other parameter setup is $M = 1000$, MCS $= 10000$, $\kappa = 0.1$.

number of groups that each player participates in is not always conducive to the promotion of cooperation.

To identify the effect of different boundary conditions on the evolution of cooperation, simulations are also carried out on the BRGG with periodic boundaries. $\rho_C$ as a function of $d$ and $\eta$ for fixed $M = 500$ and $\alpha = 1.5$ is depicted in Fig. 3(d). By comparing Fig. 3(b) and Fig. 3(d), a high level of cooperative behavior occurs only when the value of $d$ is small. It should not be overlooked that under nonperiodic boundary conditions, the number of players in the group at the network boundary is less than the average level. When $d$ is small, this gap has little effect on the results. However, as $d$ increases, this gap becomes more pronounced. In the case of the same enhancement factor $\eta$, a small number of cooperators at the network boundary can survive. As $d$ continues to increase, the gap begins to diminish, and the cooperators at the boundary need larger $\eta$ to resist the invasion of the defectors. In this case, the network is getting closer to the complete graph. This explains why cooperators and defectors can coexist under the intermediate service radius $d$. It is still necessary to clarify the rule of achieving a high level of cooperation when $d$ is small.

For small values of $d$, the fraction of cooperators $\rho_C$ as a function of the normalized enhancement factor $\eta$ for different values of $\alpha$ is shown in Fig. 4. Evidently, the cooperation will be promoted as the $\eta$ increases, no matter what the value of $\alpha$ is. Moreover, the increase in service radius $d$ is not helpful to promoting cooperation and different values of $\alpha$ can affect the final cooperation levels. In Fig. 4(a), $d$ is set to be 0.04, for a fixed $\eta$ that makes the system lies under the coexistence state of cooperators and defectors, $\rho_C$ increases with the growth of $\alpha$. Take $\eta = 0.8$ as an example, $\alpha$ changes from 0.5 to 2.0, $\rho_C$ arrives at 0.96, 0.90, 0.71, 0.11, respectively. However, as $d$ reaches 0.1, an increase in $\alpha$ will inhibit cooperation, as shown in Fig. 4(d). According to these phenomena, we speculate that the improvement of the cooperation requires the values of $z$ and $y$ to remain within a certain range.

To clearly reveal the effects of varying $\alpha$ and $d$ on cooperation, we plot $\rho_C$ as a function of the parameter $d$ for different values of $\alpha$ in Fig. 5. From Fig. 5(a)–5(d), $\eta$ is set to be 0.6, 0.7, 0.8, 0.9, respectively. As previously discovered, the cooperative behavior can be greatly enhanced when $\eta$ is varied from 0.6 to 0.9. It is notably mentioned that, the fraction of cooperators first rises rapidly until reaching a maximum value and then decreases as $d$ increases. That is, for each $\alpha$, a peak appears in the function of $\rho_C$ with respect to $d$. For a fixed $\eta$, as $\alpha$ increases, the corresponding maximum value of $\rho_C$ becomes larger, and the value of $d$ that required to reach the peak becomes smaller. These phenomena reveal that the level of cooperation will be promoted under a certain network structure with small $z$ and $y$, which validates our conjecture above.

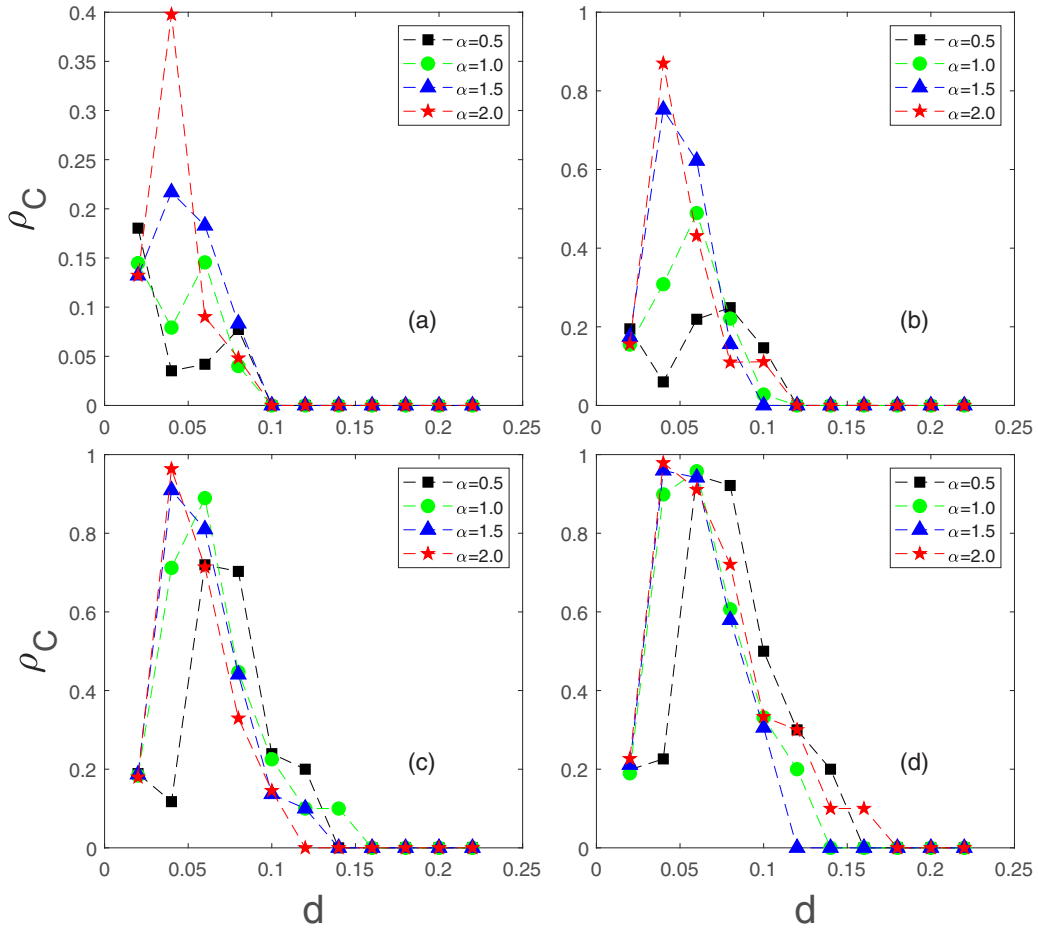


FIG. 5. Fraction of $\rho_C$ at the stationary state as a function of the service radius $d$ for different values of $\alpha$. From (a)–(d), the normalized enhancement factor $\eta$ is set to be 0.6, 0.7, 0.8, 0.9, respectively. In each panel, the $\alpha$ is changed from 0.5 to 2.0. Other parameter setup is $M = 1000$, MCS $= 10000$, $\kappa = 0.1$.

Our observations are significantly different from the conclusions that large group are advantageous to small groups, as is reported in Ref. [33] for PGGs on the square lattice where both players and public goods are depicted by one kind of nodes. Nevertheless, through a large number of empirical studies, Ostrom *et al.* [2–4] found that cooperation can be promoted in relatively small groups, which is consistent with our results. Then, why can BRGGs with relatively small values of $y$ and $z$ promote cooperation? Some intuitive explanations are given as follows: a cooperator has more chances to be infected by defectors when the group size and the number of groups he engages in is large enough, different from the cooperators in small groups that can huddle together to resist the invasion of the defectors.

Above explications can be corroborated by analyzing the microscopic process of cooperation emergence in the PGG on BRGG. We present the $\rho_C$ at each time step in Fig. 6. In Fig. 6(a), without loss of generality, $d$ is set to be 0.08. At the same time, the $\alpha$ is set to be 0.5, 1.0, 1.5, 2.0. One can see that the fraction of cooperators $\rho_C$ decline at the beginning of evolution but rise later. Compared with the public goods game on the complete graph [see the Fig. 6(b)], small groups on the BRGG promote the emergence of cooperation. This observation supports the previous explanations that due to the random initial distribution of strategies, cooperators are relatively dispersed in the network at the beginning. Under this situation, defectors infiltrate through most groups and exploit cooperators. As evolution continues,

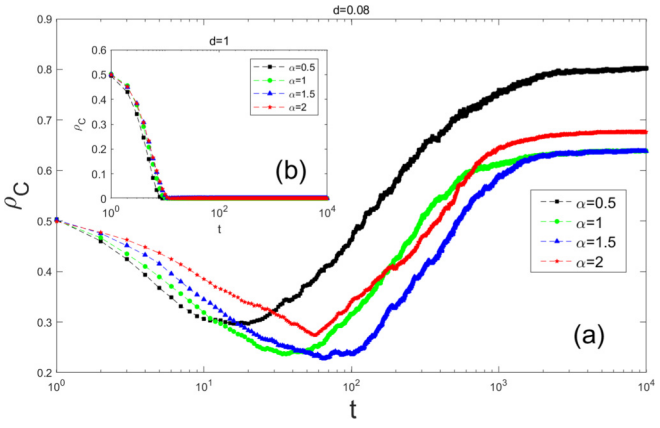


FIG. 6. Fraction of cooperators $\rho_C$ at each MCS time step. The service radius $d$ is set to be 0.08 in (a) and 1.0 in (b). In each panel, the $\alpha$ is changed from 0.5 to 2.0. Other parameter setup is $M = 1000$, MCS $= 10000$, $\kappa = 0.1$.

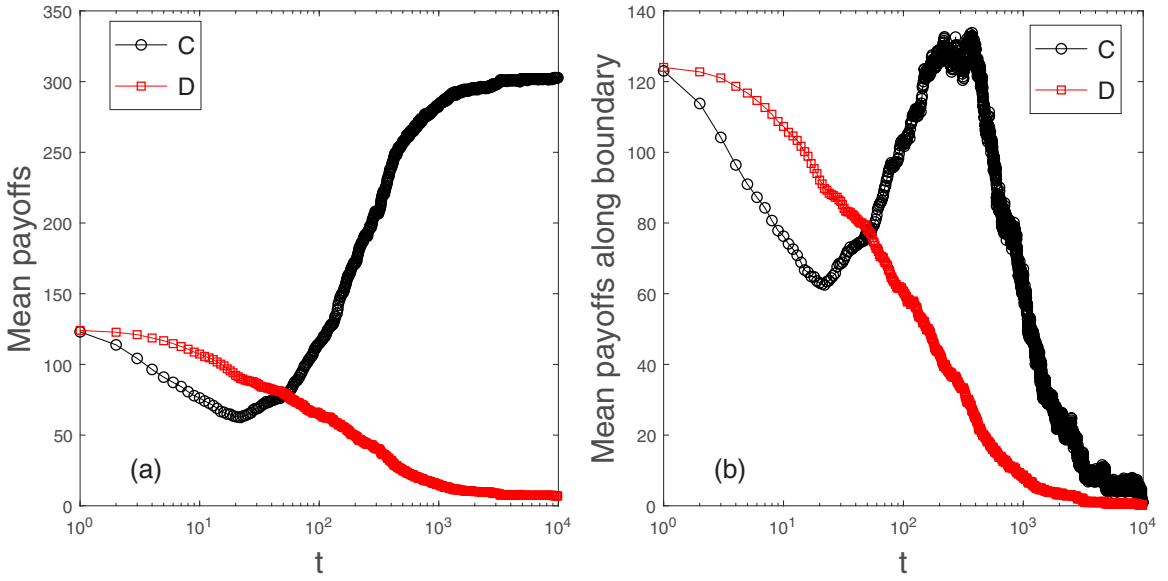


FIG. 7. (a) The mean payoffs of cooperators and defectors at each MCS time step. (b) The mean payoffs of cooperators and defectors along the boundary of the clusters. In each panel, the parameter setup is $\alpha = 1.5$, $d = 0.08$, $M = 1000$, MCS $= 10000$, $\kappa = 0.1$.

the cooperators tend to form clusters, where cooperators assist each other in avoiding defectors' exploitation in small groups. Generally speaking, the formation of the cooperator clusters influences the payoffs of cooperators and defectors. The cooperators along the boundary gradually have higher payoffs than those of defectors, which favors the spreading of cooperators.

To corroborate the above point, we illustrate the mean payoffs of cooperators and defectors as a function of time step $t$ in Fig. 7(a). Without loss of generality, we set $d = 0.08$ and $\alpha = 1.5$. In the beginning, the defectors' mean payoff is higher than that of the cooperators. As evolution continues, there are more and more defectors, leading to a decline in the profits of defectors. At the same time, the surviving cooperators begin to form clusters and obtain higher returns than the defectors, so the defectors that close to the cooperators tend to switch camps. Moreover, the mean payoffs of cooperators and defectors along the boundary as a function of time step $t$ is shown in Fig. 7(b), where a cooperator (defector) is on the boundary if it has at least one defector (cooperator) neighbor. What differs from the above results is that the mean payoffs of the cooperators along the boundary will continue to decline after rising. It stands to reason that the higher the proportion of cooperators, the more contacts between defectors and cooperators, the average income of defectors should also increase, but due to the random distribution of public goods and individuals, the degree of each individual and the number of the available public resources will inevitably be different. Of course, individuals with higher degrees participate in more public goods games and can change strategies more quickly during evolution. At the same time, more benefits can be obtained by these players according to the income accumulation rules, which are the opposite for the players with smaller degrees. Therefore, as the evolution progresses, the payoffs of the defectors and cooperators both decrease, opposite to the evolution on the square lattice where defectors' payoffs first drop and then rise [42].

## IV. CONCLUSION

In summary, we have studied the evolution of cooperation in spatial PGGs on the BRGG. Here, both individuals and public goods are placed at random locations in the unit square. Each public good has a circular service range and the players that fall into the same range form a group. In contrast with the traditional version that public goods and individuals are tightly tied together, they are independent of each other in our model. In this case, the cooperators can survive the evolution in the absence of reputation, punishment, and other mechanisms. Under nonperiodic boundary conditions, cooperation can reach a high level when $d$ is small. For the intermediate service radius $d$, cooperators and defectors can coexist in the system. Nevertheless, under periodic boundary conditions, a high level of cooperative behavior occurs only when the value of $d$ is small. Through comparison, the effect of boundary conditions on the results can be verified. Furthermore, we explore the impact brought about by the structure of BRGG on the level of cooperation. All the results indicate that cooperation is promoted when group size and the average number of groups that each person participates in (i.e., $z$ and $y$) are relatively small. In other words, increasing these parameters does not necessarily lead to the promotion of cooperation, which is the opposite of the results on the square lattice [33,43], but is consistent with the conclusions of empirical research drawn by Ostrom [3,4]. By analyzing the microscopic process of evolution, we find that cooperators can survive by forming clusters to avoid defectors' exploitation as the evolutionary process forward. We hope our research can bring inspiration for understanding the emergence of cooperation.

## ACKNOWLEDGMENTS

This work is supported by National Natural Science Foundation of China (Grants No. 71571143, No. 71671140, No.

71601156, and No. 71871180) and sponsored by the Seed Foundation of Innovation and Creation for Graduate Students in Northwestern Polytechnical University (Grants No. ZZ2019216) and the Innovation Foundation for Doctor Dissertation for Northwestern Polytechnical University (Grant No. CX201961).

[1] G. Hardin, Science **162**, 1243 (1968).
[2] M. Olson, *The Logic of Collective Action: Public Goods and the Theory of Groups*, American Studies Collection (Harvard University Press, Cambridge, 1971).
[3] E. Ostrom, Issues of definition and theory: Some conclusions and hypotheses, in *Proceedings of the Conference on Common Property Resource Management, April 21–26, 1985* (National Academy Press, Washington, DC, 1986), pp. 599–614.
[4] A. R. Poteete, M. A. Janssen, and E. Ostrom, *Working Together: Collective Cction, the Commons, and Multiple Methods in Practice* (Princeton University Press, Princeton, 2010).
[5] J. M. Smith, *Evolution and the Theory of Games* (Cambridge University Press, Cambridge, 1982).
[6] K. Binmore, Game Equilibrium Models II, 85 (1994).
[7] A. M. Colman, *Game Theory and Its Applications: In the Social and Biological Sciences* (Psychology Press, Abingdon, 2013).
[8] J. Hofbauer and K. Sigmund, *Evolutionary Games and Population Dynamics* (Cambridge University Press, Cambridge, 1998).
[9] H. Gintis, *Game Theory Evolving: A Problem-Centered Introduction to Modeling Strategic Behavior* (Princeton University Press, Princeton, 2000).
[10] M. A. Nowak, *Evolutionary Dynamics* (Harvard University Press, Cambridge, 2006).
[11] G. Szabó and G. Fath, Phys. Rep. **446**, 97 (2007).
[12] A. E. Roth and J. H. Kagel, *The Handbook of Experimental Economics*, Vol. 1 (Princeton University Press, Princeton, 1995).
[13] K. Sigmund, *The Calculus of Selfishness*, Vol. 6 (Princeton University Press, Princeton, 2010).
[14] C. Hauert and G. Szabo, Complexity **8**, 31 (2003).
[15] C. Hauert, S. De Monte, J. Hofbauer, and K. Sigmund, Science **296**, 1129 (2002).
[16] C. Hauert, S. De Monte, J. Hofbauer, and K. Sigmund, J. Theor. Biol. **218**, 187 (2002).
[17] D. Semmann, H.-J. Krambeck, and M. Milinski, Nature (London) **425**, 390 (2003).
[18] H. Brandt, C. Hauert, and K. Sigmund, Proc. Natl. Acad. Sci. **103**, 495 (2006).
[19] J.-Y. Guan, Z.-X. Wu, and Y.-H. Wang, Phys. Rev. E **76**, 056101 (2007).
[20] Z.-G. Huang, S.-J. Wang, X.-J. Xu, and Y.-H. Wang, Europhys, Lett. **81**, 28001 (2007).
[21] H.-X. Yang, W.-X. Wang, Z.-X. Wu, Y.-C. Lai, and B.-H. Wang, Phys. Rev. E **79**, 056107 (2009).
[22] A. Li, T. Wu, R. Cong, and L. Wang, Europhys, Lett. **103**, 30007 (2013).
[23] Y. Zhang, T. Wu, X. Chen, G. Xie, and L. Wang, J. Theor. Biol. **334**, 52 (2013).
[24] M. A. Nowak and R. M. May, Nature (London) **359**, 826 (1992).
[25] C. Hauert and M. Doebeli, Nature (London) **428**, 643 (2004).
[26] F. C. Santos, J. M. Pacheco, and T. Lenaerts, Proc. Natl. Acad. Sci. **103**, 3490 (2006).
[27] M. Perc and A. Szolnoki, BioSystems **99**, 109 (2010).
[28] A. Szolnoki, M. Perc, and G. Szabó, Phys. Rev. E **80**, 056109 (2009).
[29] M. A. Nowak, Science **314**, 1560 (2006).
[30] G. Szabó and C. Hauert, Phys. Rev. Lett. **89**, 118101 (2002).
[31] F. C. Santos, M. D. Santos, and J. M. Pacheco, Nature (London) **454**, 213 (2008).
[32] Z. Rong and Z.-X. Wu, Europhys. Lett. **87**, 30001 (2009).
[33] A. Szolnoki and M. Perc, Phys. Rev. E **84**, 047102 (2011).
[34] M. Barthélemy, Phys. Rep. **499**, 1 (2011).
[35] J. Dall and M. Christensen, Phys. Rev. E **66**, 016121 (2002).
[36] M. Penrose *et al.*, *Random Geometric Graphs*, Vol. 5 (Oxford University Press, Oxford, 2003).
[37] U. Alon, I. Balberg, and A. Drory, Phys. Rev. Lett. **66**, 2879 (1991).
[38] G. Szabó and C. Tőke, Phys. Rev. E **58**, 69 (1998).
[39] G. Szabó and J. Vukov, Phys. Rev. E **69**, 036107 (2004).
[40] J. Y. Wakano, Math. Biosci. **201**, 72 (2006).
[41] H. Hinrichsen, Adv. Phys. **49**, 815 (2000).
[42] D.-M. Shi, H.-X. Yang, M.-B. Hu, W.-B. Du, B.-H. Wang, and X.-B. Cao, Physica A **388**, 4646 (2009).
[43] R. M. Isaac, J. M. Walker, and A. W. Williams, J. Pub. Econ. **54**, 1 (1994).